



Production of Sustainable Building Materials Incorporating Electric Arc Furnace Dust and Meta-Kaolin

**Moataz Ahmed Ali Kelany^{1*}, Abdeen Mohamed Abd El Halim Attia El Nagar²,
Hisham Moustafa Mohamed Khater², Mohamed Ahmed Rashed³
and Sawsan Mohamed Said Haggag³**

¹*Department of Chemistry, Ezz El Dekheila Steel Company, Alexandria, Egypt.*

²*Department of Housing and Building, National Research Center (HBRC), Cairo, Egypt.*

³*Faculty of Science, Alexandria University, Egypt.*

Authors' contributions

This work was carried out in collaboration among all authors. All authors read and approved the final manuscript.

Article Information

Editor(s):

(1) Dr. Sandeep Rai, Shroff S.R. Rotary Institute of Chemical Technology, India.

Reviewers:

(1) Mikrajuddin Abdullah, Bandung Institute of Technology, Indonesia.

(2) SeyedAli Ghahari, Purdue University, USA.

Complete Peer review History: <https://www.sdiarticle4.com/review-history/72927>

Original Research Article

**Received 18 June 2021
Accepted 28 August 2021
Published 03 September 2021**

ABSTRACT

Electric-arc furnace dust (EAFD) is an industrial waste, which generated through the volatilization of metals during reduced iron and melting of scrap during electric arc furnaces process. Utilization of EAFD consisting of hazardous metals such as Pb, Cd, Cr or Zn using the technology of geopolymerization that is illustrated in this paper. Mixing between EAFD waste and meta-kaolin (MK) have been processed to study the potential of geopolymers as waste stopping agents. Alkali activators, which are used in this paper are sodium hydroxide (NH), sodium silicate (NS). The assessment of optimum ratio specimen of added EAFD are done by replacement of various ratio of EAFD "0, 20, 40, 60 & 80" % with MK. Results of compressive strength of geopolymer samples increases with EAFD up to 60% and decreases with additional increasing of dust at all curing times: 7, 14, 28 & 90 days, respectively. FTIR, SEM, XRD were used to evaluate the optimization of EAFD in geopolymer formation.

*Corresponding author: Email: mkelany@ezzsteel.com.eg, makelany91@gmail.com;

Keywords: Geopolymer; electric arc furnace dust; metakaolin; alkali; activator.

1. INTRODUCTION

Creating and applying the term “geopolymer” was done by Davidovits “French scientist” in 1979 to represent a type of inorganic polymer with SiO_4 and AlO_4 tetrahedra being the structural units [1]. Geopolymers are inorganic molecules of huge size formed by amorphous 3D networks of tetrahedral alternately bonded by units of silicates (SiO_4) and aluminates (AlO_4) [2]. Geopolymers are synthesized from abundant minerals augmented of aluminosilicates such as (e.g. metakaolin, fly ash, and slag). Geopolymers are formed by reaction between an alkaline solution (e.g. sodium hydroxide and sodium silicate) and an aluminosilicate. Researches in geopolymers are initially focused on their applications as alternative cement to ordinary Portland cements [3]. Chemical bonding in ordinary Portland cement (OPC) differs from geopolymer in that OPC is formed by reaction hydration of calcium oxide and silicon dioxide to form calcium-silicate hydrates [4] while geopolymers are formed by polycondensation of Al and Si species reaction using alkaline solutions at temperatures lower than 60 °C, without generation of CO_2 during its synthesis, so geopolymer can be considered sustainable and environmentally friendly building materials [5,6]. Geopolymers concrete have many properties versus conventional concrete such as: higher rate of early strength gain in compressive strength, indirect tensile strength typically higher for similar compressive strength, slimmer to higher depending on alkali activator in flexural strength, lower in modulus of elasticity, lower in density, lower or similar Poisson's ratio [7,8].

Binders of geopolymer display technological and ecological features over OPC, leading to wide application of concretes for high performance building materials [9]. Alkali metal hydroxides, carbonates and silicates have been used as an alkaline solutions over the past periods alkali activated binders production [10].

Electric-arc furnace dust (EAFD) is an industrial hazardous waste, which generated through the volatilization of metals during reduced iron and melting of scrap during electric arc furnaces process. EAFD is categorized as a hazard material due to contain zinc element based on Basel Convention. Currently, EAFD represents environmental risk for most of steel industry due to obstacles of its recycling. Accordingly, EAFD

threats most of steel industrials to get environment complaint or penalties from environmental legal affairs. Therefore, geopolymer technology may be one of the proper recycling method of EAFD, which are proved in this paper and enhancing the environmental emissions with other industries by decreasing CO_2 emissions that are caused in global warming. Electric arc furnaces (EAFs) are the means of recycling steel scrap [11]. Direct Reduced Iron “DRI” and Scrap as input materials are melt into electric arc furnace by means of electric power that is applied to EAF through graphite electrodes, during melting oxygen is injected into molten steel to accelerate melting and saving of electric power consumption.

Large amount of steel are contained in steel scrap, which has been protected against corrosion by coating it with a thin layer of zinc. The coating process is means as galvanizing. When the galvanized steel is melted in EAF, zinc, together with a number other of volatile elements such as lead and cadmium, is vaporized. In a typical EAF steel-making process, the melt turbulence and high temperatures cause 1 to 2 % of the charge to be vaporized. Reaction between the vapors and oxygen are occurred and condensed on particles that are carried out of the bath by the furnace off-gases. The principal components of EAF dust are zinc and iron compounds. It is in the form of very fine powder or pelletized forming major part of the smoke or fume from the furnace as shown in Fig. 1. EAFD consists mostly of iron oxide (approx. 50/mass %) and zinc oxide (approx. 21/mass %). Other constituents include: oxides of calcium, magnesium, zinc, silicon, nickel, chromium, Lead, etc. Around 3,000,000 tonnes of EAF dust are generated worldwide every year. Many EAFD treatment processes in past decades have been investigated, but a process that is sufficiently attractive economically, technically and environmentally has not eventuated.

Metakaolin regards an anhydrous calcined form, which produced from the clay mineral kaolinite. China clay or kaolin minerals are known, which minerals rich in kaolinite and used in the porcelain manufacture, traditionally. The metakaolin particle size is smaller than the particles of cement, while not as fine as silica fume. Interlayer cations or interlayer water that are not contain in the clay mineral kaolinite. The

dehydroxylation temperature determines based on the structural layer stacking order. Between of 750 and 800 °C, disordered kaolinite dehydroxylates are occurred [12]. The kaolin dehydroxylation to metakaolin is an endothermic process results the large amount of energy that required to remove the chemically bonded hydroxyl ions. Kaolinite transforms into metakaolin above the temperature range of dehydroxylation, a complex amorphous structure, which retains some long-range order due to layer stacking [13]. A lot of the aluminum octahedral layer coordination becomes tetrahedrally and pentahedrally [14]. The nearly complete of dehydroxylation must be reached without overheating to produce a pozzolan (supplementary cementitious material), i.e., thoroughly roasted but not burnt. This lead to an amorphous, highly pozzolanic state, while sintering can caused by overheating to form a dead burnt, nonreactive refractory, having mullite and a defect Al-Si spinel [15]. In comparing to other clay minerals kaolinite displays a broad temperature interval between dehydroxylation and recrystallization, much preferring the formation of metakaolin and the thermally activated kaolin clays used as pozzolans. Also, due to the octahedral layer is directly exposed to the interlayer, structural disorder is reached more easily upon heating.



Fig. 1. Image of EAFD

Khater, M. [16] studied the impact of electric arc furnace slag (EAFS) on properties of geopolymer composites producing. He studied different quantities influence of EAFS and cement kiln dust to assess the optimum ratio by EAFS adding. He investigated that the results of compressive strength of geopolymer mortar specimens increased with EAFS up to 50% and decreased with adding of slag increase, results an increased mechanical strength than the control by 7.94%, 23.9%, 80.8% and 17.8% at ages of 90 days and 9.49, 32.03, 89.68 and 37.6% at 120 days for replacement by 10, 25, 50 and 75% of EAFS,

respectively. The increased with EAFS leads to enhance in strength with curing time.

Massarweh, O. [17] studied the utilization of EAFD through a concrete set retarder development. The efficiency of retardation up to 6 % EAFD, by cement weight, which was assessed in comparing to other two commercial retarders. The addition impact of EAFD on the hydration heat, slump retention and compressive strength was assessed. The data of experimental showed that the effectiveness of EAFD was achieved by increasing the initial and final setting time. The data of calorimetry showed that the delay of cement hydration was occurred due to the EAFD addition. EAFD or the commercial retarders did not adversely affect the concrete compressive strength at 28 days and it was in the range of 46.5 MPa to 50.7 MPa. They investigated that the solid retarder performance developed using EAFD was able to be compared to the commercial retarders. EAFD using as a retarder would result in environmental, technical and economic benefits.

Hodhod, O. [18] prepared mixes of geopolymer having metakaolin with other pozzolanic materials such as silica fume and fly ash to enhance workability and strength. Fifteen mixes were executed to study the using impact of metakaolin on physical and mechanical properties. Results showed that the mixes of geopolymer can be utilized as an effective binding material. It could be cost effective in producing brick units. The ideal of metakaolin addition mixes was 10 % as the resistance of the geopolymer bricks reached values up to 250 kg/cm².

Ghahari, S. [19] investigated to determine new sustainable materials to have fracture toughness of cement paste for example the cellulose nanocrystals (CNCs) is worthwhile. They have less environmental risks and safety due to their less toxicity. The cement paste hydration properties reinforced with cellulose nanocrystal particles, the fracture behavior, compressive strength were investigated. A three-point bending moment test, a calorimetry and thermogravimetric analysis, scanning electron microscopy (SEM), and energy dispersive x-ray spectroscopy (EDX) analysis were assessed at the age of 3, 7, and 28 days on the water-to-binder-weight ratio of 0.35 cement paste, having 0.0%, 0.2%, and 1.0% volume cellulose nanocrystals. Results showed that the compressive strength and fracture properties

were enhanced concerning the sample having 0.2 % CNCs. Initial results refer that the enhancement of CNCs can be achieved the fracture behavior of cementitious materials and can be regarded as a renewable and sustainable material in construction.

Jassim M. [20] studied the thermal decomposition of aluminum sulfate by extracting it from metakaolin through precipitation during drying and calcining process, which occurred at 800, 850, 900 and 1000 °C. The properties of crystallinity and phase of the synthesized for the assignment of calcined samples were determined by X-ray diffraction measurements, paving the temperature at the aluminum sulfate is changed to γ -alumina nano particles. The purity of alumina nanoparticle 98.81% was achieved by aluminum sulfate calcination at 1000 °C for 2 hour. BET measurement was used to assess the specific surface area, pore volume and pore size for γ -alumina nano particles. Also the particles size were calculated by BET measurement to be about 12 nm. The study showed that the kaolin might be a capable material for the γ -alumina preparation.

The aim of the present paper is to investigate the influence of adding of different ratios of electric arc furnace dust mixing with metakaolin an calcium hydroxide $\text{Ca}(\text{OH})_2$ in alkali activators to reach the optimum ratio of electric arc furnace dust to be sustainable building materials and study their impact on the mechanical and microstructural properties.

2. EXPERIMENTAL PROCEDURES

2.1 Materials

Materials that used in this investigation are electric arc furnace dust collected from Ezz El Dekhila steel company "EZDK" and Metakaolin material produced from Kaolinitic sandstone deposits existed in south Sinai. The raw materials chemical compositions are shown in Table 1. EAFD consists mostly of zinc oxide and iron oxide and other constituents as oxides of calcium, magnesium, Zinc, silicon, nickel, chromium, Lead, etc. Kaolin contains hydroxyl ions that are strongly bonded to the aluminosilicate framework and can only be altered by the temperature at 800 °C for 2 hrs to be metakaolinite. Thus, rearranging the atomic structure to form a partly ordered system with a

great reaction potential to alkaline solutions. The main chemical compositions of Kaolin and the studied metakaolin is SiO_2 and Al_2O_3 .

The mineralogical composition is showed in Fig. 2; where electric arc furnace dust material consist of magnetite, laurionite and minor content of zincite, franklinite and hyrozincite. The kaolin and metakaolin materials are composed of Kaolinite, anatase and quartz, However, metakaolin is almost amorphous and free of kaolin.

2.2 Experimental Section

Geopolymer composite mortars were made by mixing the used raw materials of each mixture (passed through a 90- μm sieve) with the alkaline activator solution sodium hydroxide for 10 min, and a further mixing for 5 min using a mixer was applied. Mortar ratio (1:1) (sand: binder materials), where binder materials are MK, Calcium hydroxide $\text{Ca}(\text{OH})_2$ and EAFD. All mixes use alkali activators, which are 10 molar of sodium hydroxide mixed with the same equal ratio of sodium silicate. In Table 1, mix design is illustrated. The used water to binder ratio was 0.50 by mass. EAFD was added to the binding material in different ratios from 0 up to 80 %, mixed well with part of the total water using a magnetic stirrer. The mortar mixture was casted into 25x25x25 mm cubic- shaped moulds, vibrated to achieve a suitable compaction then sealed with a lid to minimize any loss of evaporable water. Each mix ratio of mortar had 12 samples, which were used in experimental analysis: FTIR, XRD, compressive strength and SEM tests. All made specimens were left to be cured undisturbed at 23 °C lab temperature for 24 hrs and then subjected to a curing temperature of 40 °C with a 100 % relative humidity till 90 days.

At the end of the curing regime, the compressive strength measurements were executed to the geopolymer mortar specimens after end of the curing regime. The resulted crushed specimens were subjected to hydration process stopping by using alcohol/acetone (1:1) as a stopping solution then washing with acetone as suggested by different investigators [21,22] to prevent further hydration. For further analysis of the crushed specimens followed by drying for 24 hr at 80 °C, after that conserved in a well tight container until the time of testing.

Table 1. Chemical composition of starting materials (mass %)

| Element (%) | LOI | Na₂O | MgO | Al₂O₃ | SiO₂ | P₂O₅ | SO₃ | Cl⁻ | K₂O | CaO | TiO₂ | Cr₂O₃ | Fe₂O₃ | Co₃O₄ | Ga₂O₃ | NiO | SrO | Total |
|--|------------|------------------------|------------|------------------------------------|------------------------|-----------------------------------|-----------------------|-----------------------|-----------------------|------------|------------------------|------------------------------------|------------------------------------|------------------------------------|------------------------------------|------------|------------|--------------|
| Kaolin | 12.9 | 0.107 | 0.175 | 33.1 | 48.5 | 0.12 | 0.17 | 0.07 | 0.15 | 0.45 | 2.53 | - | 1.56 | - | 0.01 | - | 0.02 | 99.84 |
| Metakaolin (MK) | 1.08 | 0.14 | 0.44 | 38.3 | 54.8 | 0.12 | 0.26 | 0.02 | 0.05 | 0.38 | 2.61 | 0.07 | 1.59 | 0.01 | - | 0.02 | 0.01 | 99.91 |
| Element (%) | Fe | Zn | Ca | Mg | Si | Mn | Pb | Al | K | Cu | S | Cr | Ti | P | O | | | Total |
| Electric Arc Furnace Dust (EAFD) | 35 | 16.5 | 8.5 | 2.8 | 2.5 | 1.6 | 1.1 | 0.8 | 0.4 | 0.3 | 0.2 | 0.1 | 0.1 | 0.1 | 29.7 | - | - | 99.7 |

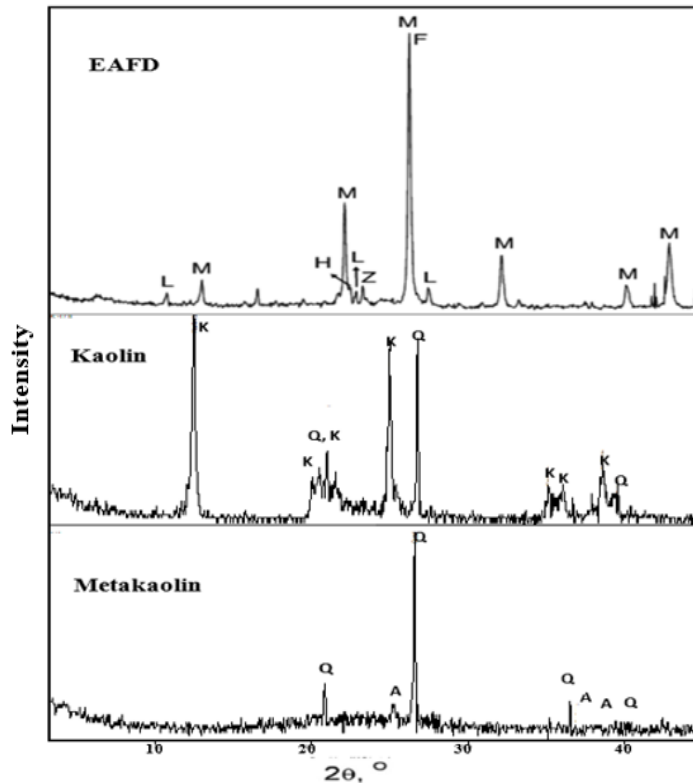


Fig. 2. X-ray diffraction patterns of EAFD, Kaolin and MK materials. [M: Magnetite (Fe_3O_4) F: Franklinite ($ZnFe_2O_4$), L: Laurionite ($Pb(OH)Cl$), Z: Zincite (ZnO), H: Hydrozincite ($Zn_5(CO_3)_2(OH)_6$), K: Kaolinite ($Al_2O_3 \cdot 2SiO_2$), A: Anatase (TiO_2)]

Table 2. The studied mixes composition containing EAFD and MK materials in the alkaline medium

| Mix | MK, % | EAFD, % | Ca(OH) ₂ , % | Activator |
|-----|-------|---------|-------------------------|--------------------------------------|
| A0 | 90 | 0 | 10 | 10 M of NH ₄ ⁺ |
| A1 | 70 | 20 | 10 | equal ratio of NS |
| A2 | 50 | 40 | 10 | |
| A3 | 30 | 60 | 10 | |
| A4 | 10 | 80 | 10 | |

2.3 Method of Investigation

Chemical analysis for geopolymer specimens was determined by XRF Sequential Spectrometer (Model: Axios Fast), which has analysis more than 1000 samples in a 24 hour period. In the compressive strength testing, a five-ton German Bruf pressing machine with a loading rate of 100 kg/min determined according to ASTM C109-13 was utilized [23]. The microstructure of hardened alkali activated electric arc furnace dust was investigated using a SEM fitted with an Inspect S model with an energy dispersive X-ray analyzer (EDX). The

progressed hydration stopping was accomplished by exposing the crushed samples to alcohol/acetone mix as suggested by different investigators [21,24]. The bonding properties of alkali-activated specimens were investigated using a Jasco- 6100 Fourier transformed infrared spectrometer (FTIR; Varian model Excalibur FTS 3000MX, Palo Alto, CA). The wave number varied between 400 and 4,000 cm^{-1} . Using a mortar and pestle, the powder samples were mixed with KBr to create the testing samples. The combination was then crushed for 20 seconds at less than 10 tonnes to form a solid pellet, which was then tested [25,36].

3. RESULTS AND DISCUSSION

3.1 Effect of Replacement of Meta-Kaolin by Electric arc Furnace Dust Precursor

FTIR spectra of 90 days cured (40°C and 100% RH) geopolymer specimens having mix composition of MK and EAFD are represented in Fig. 3. Bands description are as follow: Stretching vibration was done for O-H bond at about 3500, 1600 cm^{-1} , stretching vibration of CO_2 located at about 1405 cm^{-1} , asymmetric stretching vibration (Si-O-Si) at about 1125 cm^{-1} , asymmetric stretching vibration (T-O-Si) at about 970 cm^{-1} where T=Si or Al, symmetric

stretching vibration of CO_2 at about 860 cm^{-1} , symmetric stretching vibration (Si-O-Al) at about 740 cm^{-1} symmetric stretching vibration (Si-O-Si) in the region 570-670 cm^{-1} and bending vibration (Si-O-Si and O-Si-O) in the region of 440-570 cm^{-1} .

The figure showed the increased broadness of asymmetric band at about 970 cm^{-1} with EAFD up to 60% (A3) in addition to the shifting to lower wave number, reflecting the increased dissolution of the silica as well as increase in the glassy component. The asymmetric band at about 1125 cm^{-1} for non-solubilized silica decreased with replacement up to 60% EAFD

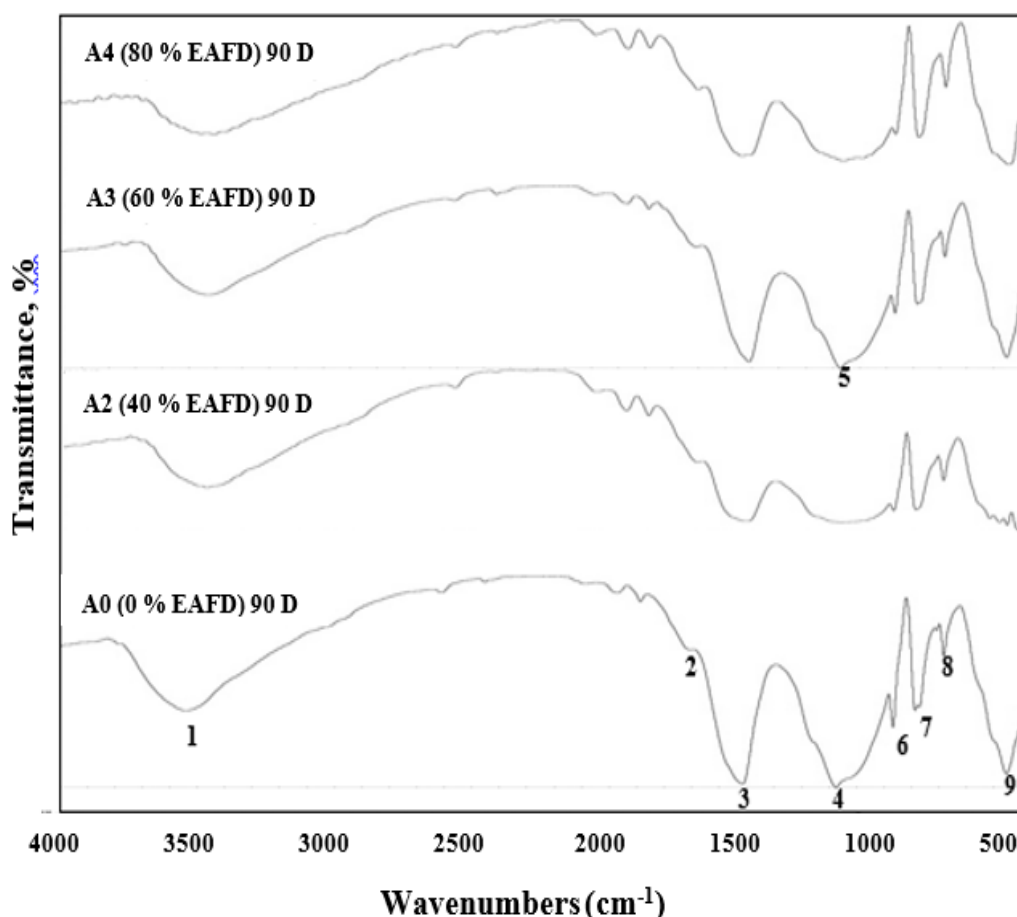


Fig. 3. FTIR spectra of 90 days geopolymer mortar specimens containing different ratios of EAFD mixed with MK at 10 Molar of alkali activators. [1: Stretching vibration of O-H bond, 2: Bending vibrations of (HOH), 3: Stretching vibration of CO_2 , 4: Asymmetric stretching vibration (Si-O-Si), 5: Asymmetric stretching vibration (T-O-Si); 6: Symmetric stretching vibration of CO_2 ; 7: Symmetric stretching vibration (Si-O-Al); 8: Symmetric stretching vibration (Si-O-Si); 9: Bending vibration (Si-O-Si and O-Si-O)]

reflecting the increased dissolution of inactive silica, while further increase leads to increase the cement of non-solubilized silica and so lower intensity of the formed geopolymer as seen clearly from the pattern. The increased intensity of the Si–O–Si asymmetric band in addition to the shift to lower wave number from 1125 to 970 cm^{-1} with increased contents of EAFD up to 60% (A3) suggests variation in aluminosilicate framework geopolymer composite resulting from cationic replacement in non-framework sites [27].

Also the increased intensity of the asymmetric stretching band at 970 cm^{-1} with EAFD at 60% (A3) refers to the amorphous content of N-A-S-H gel, which has a positive impact enhancement on the mechanical properties of the resulting structure where the promotion of aluminosilicate polycondensation reactions were done with EAFD adding increased up to 60% [28]. Using 60% EAFD (A3) lead also to an increase in the two hydration bands at about 3500, 1600 cm^{-1} , where EAFD with high hydration modulus ratio can result in high dissolution in their cationic species formed geopolymer phases leading to an extra strength of the composite. This is comprehensible with increasing of hydration band intensity. The vibration band was bended at about 440-570 cm^{-1} increases also with EAFD % increasing [29].

The bands, which are appeared in the regions of 1405 cm^{-1} (ν C–O), and 860 cm^{-1} (δ C–O) are typical of CO_3^{2-} vibrational groups existing in inorganic carbonates. The carbonate intensity resulted increased from the used raw materials as well as carbonation of free unreacted alkalis [30].

X-ray diffraction spectra for geopolymers containing 0 %, 40 % 60 % and 80 % ratios of EAFD mixed with MK at the age of 90 day are shown in Fig. 4. The mineralogical pattern showed that there is an amorphous region at 6 ° to 10 ° 2 θ for aluminosilicate gel with quite small band for amorphous phases in geopolymer at the zone from 17 ° to 34° 2 θ . Those regions are known as the important characterization regions for geopolymer, wherever the evolution of these regions will influence performance of the produced composite [31]. It is interested to note that CSH peaks are detected at EAFD ratios (40, 60, 80) % (A2, A3 & A4) respectively, but it is not detected at EAFD ratio 0% (A0). There is an increase in intensity of CSH peaks by increasing EAFD ratio up to 60% (A3). The CSH peak was detected at 60% of EAFD (A3) and 40% EAFD

(A2) at (28.7 °, 31.2 °, 32.7 ° & 40.04 °) 2 θ and it was detected at 80 % of EAFD only at at (28.7 °, 31.2 ° & 40.04°) 2 θ , but it was not detected at reference sample 0 % EAFD (A0).

This broad hump may indicted that the quantity of amorphous geopolymer gel produced increasing by adding EAFD up to 60% (A3), while further increase in EAFD results in the increased crystalline phases which cannot be dissolved by the added alkali [32,33].

The results of compressive strength for geopolymer specimens mixes along with various EAFD ratios and MK cured at 100 % relative humidity and 40°C up to 90 days are shown in Fig. 5. In general, the degree of polymerization is represented by the geopolymers compressive strength that is strongly affected by the soluble aluminates and silicates of the geopolymeric system.

As can be seen in Fig. 5, the results displayed that the compressive strength decrease up to 40 %, followed by an increased strength up to 60 %. The first decrease in strength results from imbalance of matrix structure with 40 % replacement, while the following increase up to 60 %, results from the increased CSH formation as well as geopolymer structure as 60 % replacement leads to enhancement in the matrix structure and balancing the three dimensional network by free dissolved cations. Further increase in EAFD, results in an increased crystalline phases as well as the increased iron content with lower the driving force for geopolymer reaction by precipitation as iron hydroxide. So the intensity of the formed amorphous geopolymer decreased as confirmed by XRD & FTIR patterns in Fig. 3 and Fig. 4, respectively. The increase up to 60% EAFD reflects the increased growth of amorphous content in addition to the high hydration modulus of EAFD ratio 60% (A3), which depicts increasing of CSH peaks with EAFD ratios up to 60% (A3) and the broad hump was observed at 17 ° to 35 °2 θ at 60% EAFD (A3) compared with the reference sample 0% EAFD (A0) as well as EAFD ratios (40 & 80) %. FTIR also depicts the increased asymmetric stretching vibration at about 950 cm^{-1} for Al-O-Si for the aforementioned ratio. These broad hump as well as the asymmetric vibration band illustrate the increased amorphous geopolymer gel by adding EAFD up to 60% (A3). The reduction in compressive strength which was observed at EAFD ratio 20% (A1) resulted 18 MPa at 90 day,

it was expected due to the retardation influence enforced on the hydration reaction in the zinc "Zn" content of EAFD [34]. It is noted that the

improvement in compressive strength increases with adding of EAFD with the time of curing [33,35].

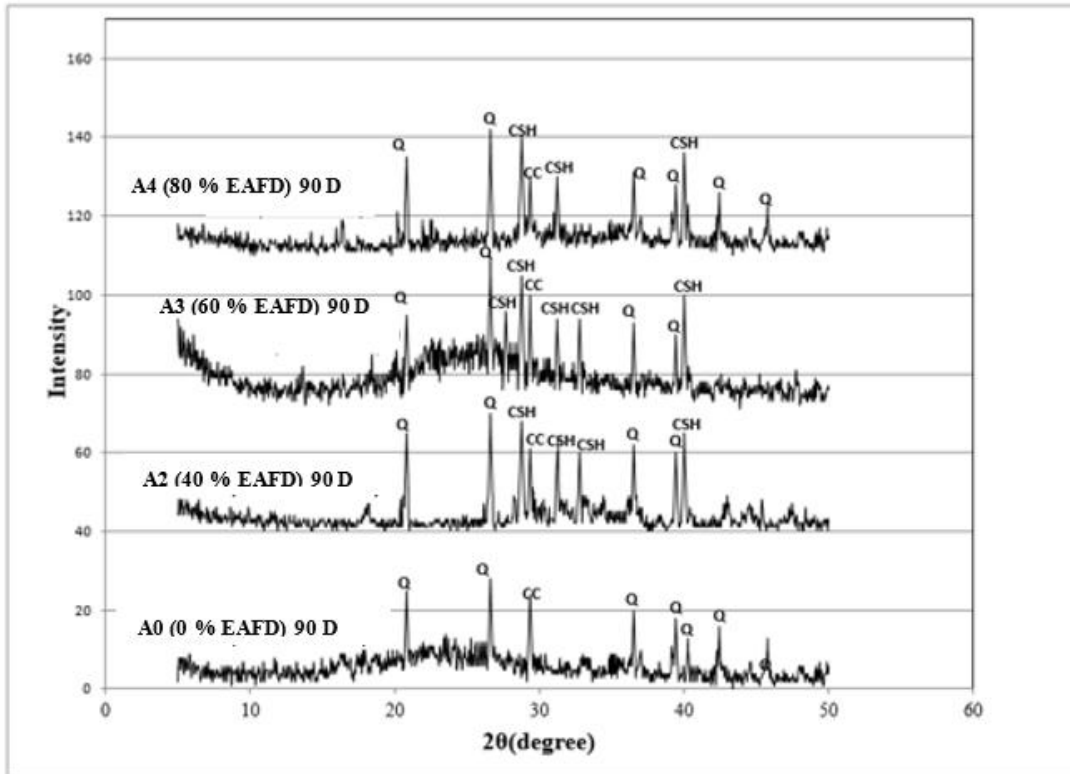


Fig. 4. X-ray diffraction patterns of 90 day geopolymer specimens having various ratios of EAFD mixed with MK at 10 Molar of alkali activators. [Q: Quartz, CC: Calcium Calcite, CSH: Calcium Silicate Hydrate]

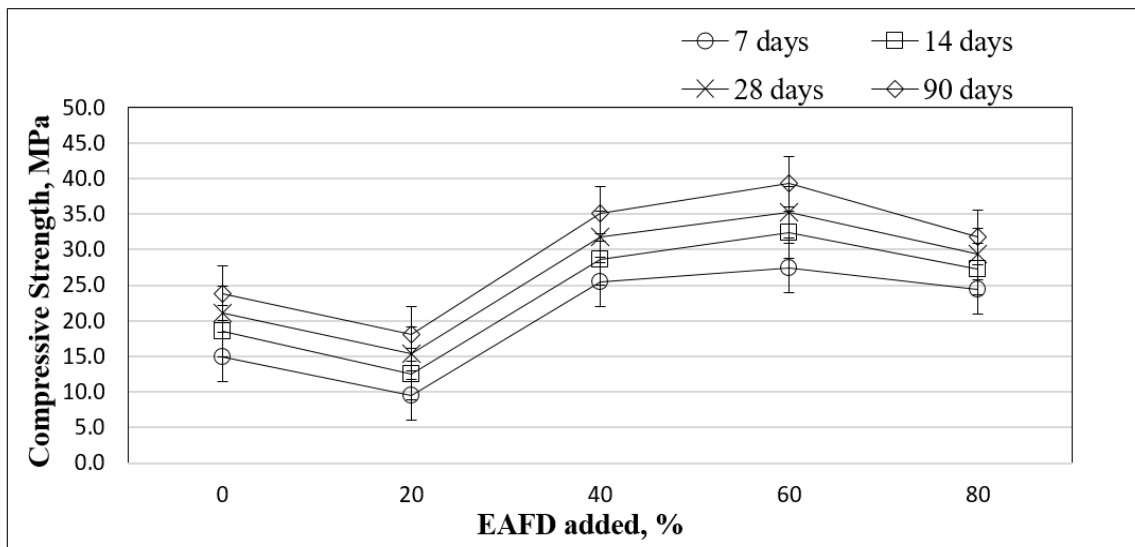


Fig. 5. Compressive strength of alkali activated MK geopolymer specimens having various dosages of EAFD.

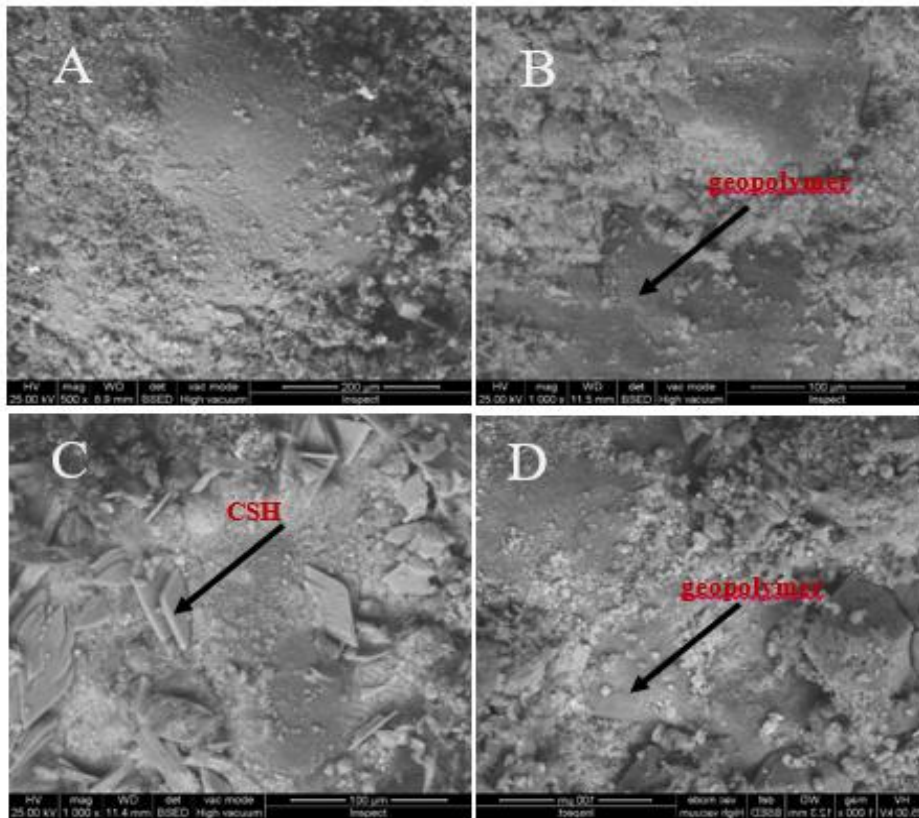


Fig. 6. SEM micrographs of 90 days geopolymer specimens having various ratios of EAFD mixed with MK at 10 Molar of alkali activators. [A] A0: 0 % of EAFD, B) A2: 40 % of EAFD, C) A3: 60 % of EAFD, A) D4: 80 % of EAFD]

It is illustrated by the high alkali content in EAFD that leads to the increase of medium pH and so the polymerization degree of the resulting product, also EAFD is much harder than MK due to the high iron content as represented in Table 1 [28]. The combination impact of 60% EAFD (A3) mixed with 30% MK and 10% of calcium hydroxide $\text{Ca}(\text{OH})_2$ expected that causes a higher strength resulted 39 MPa at 90 day since the EAFD anhydrous part contributes strongly to strength as compared to MK grains [30]. It is also expected that is attributed to the fact that Ca^{2+} , Fe^{3+} are capable of acting as charge-balancing cations within the geopolymeric binder structure [36].

The SEM microstructure of 90 days cured geopolymer specimens having 0, 40, 60 & 80% ratios of EAFD (A0, A2, A3 & A4) respectively mixed with MK & calcium hydroxide $\text{Ca}(\text{OH})_2$ at 10M of NH mixed with the same equal weight of NS is shown in Fig. 6.

The micrographs of various ratios % of EAFD show geopolymer plates dispersing within the

structure adding to calcium silicate hydrate CSH that consisted by the interaction of free dissolved silica with free calcium oxide in EAFD as well as free dissolved calcium species within the composites forming CSH which increase the binding properties of three dimensional of geopolymer structure. Further increasing in the EAFD results up to 60% (A3), results increase in the CSH as shown in (Fig.6-C). It is also noted that clarity of more nucleation sites leading to a homogeneous and hard structure that reflect to high mechanical strength [37]. The elucidations observed from SEM confirms the growth of compressive strength up to 60% followed by strength decrease [38].

4. CONCLUSION

EAF dust usage can be successfully used up to 60%, but further increase leads to an iron content increase that will precipitate as hydroxide and lower the medium alkalinity. 60% of EAFD used results in the amorphous content growth of N-A-S-H gel and the binding gels (C-(A)-SH). The compressive strength results increase of

geopolymer mortar specimens is conducted with EAF dust up to 60% then decreases with further dust increase at all curing times: 7, 14, 28, & 90 days, respectively. The results showed the possibility of incorporation of high content of EAFD up to 60% in the formation of sustainable building materials.

COMPETING INTERESTS

Authors have declared that no competing interests exist.

REFERENCES

- Davidovits J. Geopolymer chemistry and properties. Geopolymer 88, First European Conference on Soft Mineralogy, Compiègne, France. 1988a;1:25-48.
- Davidovits J. Geopolymers - inorganic polymeric new materials. Journal of Thermal Analysis. 1991;37:1633-1656.
- Duxson P, Lukey G, Van Deventer J. Physical evolution of Na-geopolymer derived from metakaolin up to 1000°C. J. Mater. Sci. 2007;42:3044-3054.
- Provis JL, Duxson P, Van Deventer JS. The role of particle technology in developing sustainable construction materials. Advanced Powder Technology. 2010;21:2-7.
- Kisku N, Joshi H, Ansari M, Panda SK, Nayak S, Dutta SC. A critical review and assessment for usage of recycled aggregate as sustainable construction material. Construction and Building Materials. 2017;131:721-40.
- Dalawai VN, Srikanth L, Srikanth I, Arockiasamy M. Effective Utilization of Fly Ash and Steel Slag for Partial Replacement of Cement and River Sand for Sustainable Construction. In Advances in Geotechnics and Structural Engineering. Springer, Singapore. 2021;279-291.
- Shaikh FUA. Mechanical and durability properties of fly ash geopolymer concrete containing recycled coarse aggregates. International Journal of Sustainable Built Environment. 2016;5(2):277-287.
- Halim LN, Ekaputri JJ. The Influence of Salt Water on Chloride Penetration in Geopolymer Concrete. In MATEC Web of Conferences. EDP Sciences. 2017;97: 01002.
- Van Deventer JSJ, Provis JL, Duxson P, Brice DG. Chemical research and climate change as drivers in the commercial adoption of alkali-activated materials. Waste and Biomass Valorization. 2010; 1(1):145–155. Available: <http://dx.doi.org/10.1007/s12649-010-9015-9>
- Provis JL. Activating solution chemistry for geopolymers. In: Provis, J.L., van Deventer, J.S.J. (eds.) Geopolymers: Structures, Processing, Properties and Industrial Applications, Woodhead Publishing, Abingdon. 2009;50–71.
- Arnold MC, de Vargas AS, Bianchini L. Study of electric-arc furnace dust (EAFD) in fly ash and rice husk ash-based geopolymers. Advanced Powder Technology. 2017;28(9):2023–2034.
- Kakali G, Perraki T, Tsvilis S, Badogiannis E. Thermal treatment of kaolin: the effect of mineralogy on the pozzolanic activity. Applied Clay Science. 2001;20(1–2):73–80.
- Bellotto M, Gualtieri A, Artioli A, Clark SM. Kinetic study of the kaolinite-mullite reaction sequence. Physics and Chemistry of Minerals. 1995;22:207–217.
- Fernandez R, Martirena F, Scrivener KL. The origin of the pozzolanic activity of calcined clay minerals: A comparison between kaolinite, illite and montmorillonite. Cement and Concrete Research. 2011;41(1):113-122.
- Snellings R, Mertens G, Elsen J. Supplementary cementitious materials. Reviews in Mineralogy and Geochemistry. 2012;74:211–278.
- Khater HM. Influence of electric arc furnace slag on characterisation of the produced geopolymer composites. Epitoanyag-Journal of Silicate Based & Composite Materials. 2015;67(3).
- Massarweh O, Maslehuddin M, Al-Dulaijan SU, Shameem M, Ahmad S. Development of a concrete set retarder utilizing electric arc furnace dust. Construction and Building Materials. 2020; 255:119378.
- Hodhod OA, Alharthy SE, Bakr SM. Physical and mechanical properties for metakaolin geopolymer bricks. Construction and Building Materials. 2020; 265:120217.
- Ghahari S, Assi LN, Alsalman A, Alyamaç KE. Fracture Properties Evaluation of Cellulose Nanocrystals Cement Paste. Materials. 2020;13(11):2507. DOI: 10.3390/ma13112507

20. Kshash JM, Baha'a AS. Preparation of nanogama alumina from Iraqi kaolin. *Iraqi Bulletin of Geology and Mining*. 2018; 14(1):121-130.
21. Saikia N, Usami A, Kato S, Kojima T. Hydration behavior of ecocement in presence of metakaolin. *Resource Progressing Journal*. 2004;51:35–41.
22. El-Sayed HA, Abo El-Enein SA, Khater HM, Hasanein SA. Resistance of Alkali Activated Water Cooled Slag Geopolymer to Sulfate Attack. *Ceramics – Silikaty*. 2011;55(2):153-160.
23. ASTM C109M-12. Standard Test Method for Compressive Strength of Hydraulic Cement Mortars; 2012. Available:http://dx.doi.org/10.1520/C0109_C0109M
24. Taha AS, El-Didamony H, Abo El-Enein SA, Amer HA. Physicochemical properties of supersulphated cement pastes. *Zement-Kalk-Gips*. 1981;34:351–353.
25. Khater HM. Effect of cement kiln dust on Geopolymer composition and its resistance to sulphate attack. *Green Materials*. 2013;1(1):36-46. Available:<http://dx.doi.org/10.1680/gmat.12.00003>.
26. Pnias D, Giannopoulou IP, Perraki T. Effect of synthesis parameters on the mechanical properties of fly ash-based geopolymers. *Colloids and Surfaces A: Physicochemical and Engineering Aspects*. 2007;301(1-3):246–254. Available:<http://dx.doi.org/10.1016/j.colsurfa.2006.12.064>
27. Duxson P, Fernández-Jiménez A, Provis JL, Lukey GC, Palomo AJ, van Deventer. SJ Geopolymer technology: the current state of the art, *J. Mater. Sci*. 2006;42(9):2917–2933.
28. Isillsil Ozer S, Soyer-Uzun. Relations between the structural characteristics and compressive strength in metakaolin based geopolymers with different molar Si/Al ratios, *Ceram. Int*. 2015;41(8):10192–10198.
29. He J, Jie Y, Zhang J, Yu Y, Zhang G. Synthesis and characterization of red mud and rice husk ash-based geopolymer composites, *Cem. Concr. Compos*. 2013;37:108–118.
30. Lancellotti I, Catauro M, Ponzoni C, Bollino F, Leonelli C. Inorganic polymers from alkali activation of metakaolin: effect of setting and curing on structure, *J.Solid State Chem*. 2013;200:341–348.
31. Hajjaji W, Andrejkovicová S, Zanelli C, Alshaaer M, Dondi M, Labrincha JA, Rocha F. Composition and technological properties of geopolymers based on metakaolin and red mud, *Mater. Des*. 2013;52:648–654.
32. Dimas DD, Giannopoulou IP, Pnias D. Utilization of alumina red mud for synthesis of inorganic polymeric materials, *Miner. Process. Extr. Metall. Rev*. 2009;30(3):211–239.
33. Li X, Liu Y, Li W, Li C, Sanjayan JG, Duan W, Li Z. Effects of graphene oxide agglomerates on workability, hydration, microstructure and compressive strength of cement paste, *Constr. Build. Mater*. 2017;145:402–410.
34. Ng C, Alengaram UJ, Wong LS, Mo KH, Jumaat MZ, Ramesh S. A review on microstructural study and compressive strength of geopolymer mortar, paste and concrete, *Construct. Build. Mater*. 2018;186:550–576.
35. Provis JL, Lukey GC, Deventer JSJv. Do geopolymers actually contain nanocrystalline zeolites? A reexamination of existing results, *Chem. Mater*. 2005;17(12):3075–3085.
36. Görhan G, Aslaner R, Sinik O. The effect of curing on the properties of metakaolin and fly ash-based geopolymer paste, *Compos. B Eng*. 2016;97:329–335.
37. Assaedi H, Shaikh FUA, Low IM. Effect of nano-clay on mechanical and thermal properties of geopolymer. *Journal of Asian Ceramic Societies*. 2016;4(1):19-28.
38. Buchwald A, Tatarin R, Stephan D. Reaction progress of alkaline-activated metakaolin-ground granulated blast furnace slag blends. *J Mater Sci*. 2009;44:5609–5617.

© 2021 Kelany et al.; This is an Open Access article distributed under the terms of the Creative Commons Attribution License (<http://creativecommons.org/licenses/by/4.0>), which permits unrestricted use, distribution, and reproduction in any medium, provided the original work is properly cited.

Peer-review history:
The peer review history for this paper can be accessed here:
<https://www.sdiarticle4.com/review-history/72927>